2004

Effects of Low Tide Rainfall on Intertidal Zone Material Cycling

Raymond Torres

Miguel A. Goni

George Voulgaris
University of South Carolina - Columbia, gvoulgaris@geol.sc.edu

Charles R. Lovell
University of South Carolina - Columbia, lovell@biol.sc.edu

James T. Morris

Publication Info

Published in *Coastal and Estuarine Studies*, ed. Sergio Fagherazzi, Marco Marani, and Linda K. Blum, Volume 59, 2004, pages 93-114.

6

Effects of Low Tide Rainfall on Intertidal Zone Material Cycling

Raymond Torres, Miguel A. Goñi, George Voulgaris, Charles R. Lovell and James T. Morris

Sediment transport by rainfall-runoff processes is well documented for terrestrial landscapes but few studies have focused on rainfall-runoff effects in intertidal areas. Here we present geochemical analyses performed on sediment samples collected during low tide irrigation experiments, and tidal channel turbidity measurements taken during natural rainfall over North Inlet Marsh, South Carolina. Order of magnitude approximations indicate that a single 10-minute storm may entrain 8-15% of the local annual average sediment accumulation. This rainfall-entrained material is enriched in organic nitrogen and marine algal matter, and therefore of high nutritional quality. Hence, rainfall-driven material fluxes represent a potentially significant "non-point source" of carbon and nutrients to the estuarine water column. The fate of this material, however, is not known. Two natural low tide rainfall events that occurred 2.1 days apart provide insight into the role of tides on the redistribution of rainfall-entrained material. The first storm produced a ~200 fold increase in turbidity but the latter produced a ~2 fold increase. The combination of these observations with measurements of tidal hydrodynamics indicate that rainfall may erode the marsh surface, and rainfall-entrained material reaching the subtidal zone within a 2.4 hour interval preceding low tide will be subject to wider estuarine distribution, and possibly exported to the coastal ocean. Material arriving outside of that time window is likely to settle in the subtidal zone or resettle on the marsh with the next high tide. Regardless of the fate of this material, results show that rainfall-runoff processes augment biogeochemical cycling.

Introduction

A recurring but poorly understood process affecting estuarine biogeochemical cycling is low tide rainfall. During low tide, kinetic energy from raindrop impacts may perform work by ejecting sediment away from the impact area, and raindrop deformation may generate shear stresses that are sufficient to initiate movement of cohesive sediment (Figure 1), material that ordinarily is not mobilized by tidal currents or short-period surface waves. Also, resulting freshwater sheetflow may transport detached material to tidal creek networks and the subtidal environment. Consequently, low tide rainfall-runoff processes may enhance the cycling of, for example, benthic microalgae and their products, a primary carbon source for

The Ecogeomorphology of Tidal Marshes
Coastal and Estuarine Studies 59

10.1029/59CE07

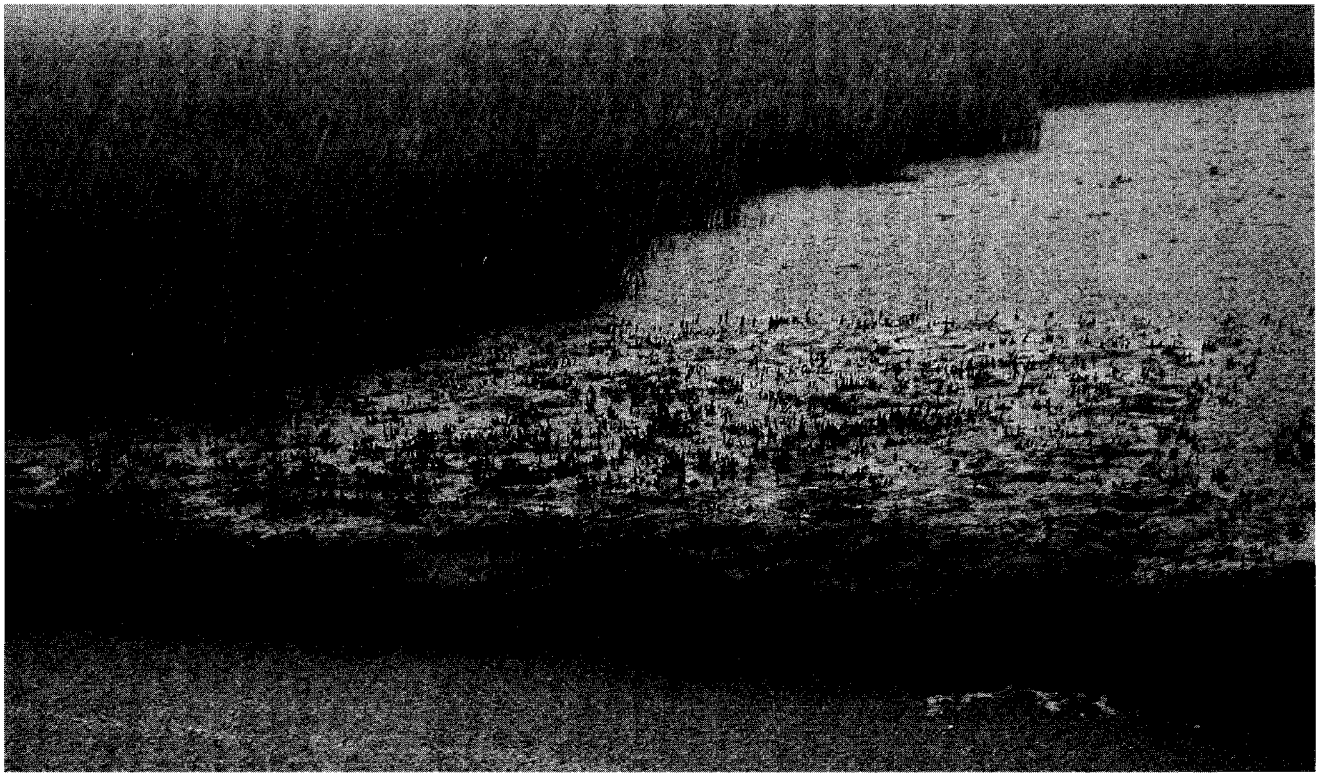

Figure 1. A low tide rainfall event at North Inlet, SC. Storm occurred on June 14, 2003 (day 165.5; Figure 5); maximum 4-minute intensity was 174 mm/hr. Turbidity sensor and rain gage are 50 m to the right. Two small rivulets at cusps in the *S.alterniflora* edge feed sediment-laden freshwater to the transient pool in the background. The muddy platform in the foreground experienced a recent *S. alterniflora* die off and dark colored stalk remnants protrude upward. The subtidal channel is flowing to the right and ebb tidal stage is approximately 0.4 m above low tide. Note discharge from the pool to the subtidal channel (near the white froth) through an incised rivulet. Exposed channel bank is approximately 5 m across.

estuarine food webs [e.g., Decho, 1988]. Although low tide rainfall-driven material cycling may be considered a short-term phenomenon, resulting material fluxes have not been well characterized, and the cumulative effects of recurring short-term rainfall events are not known. Therefore, changes in the frequency of coastal zone precipitation due to expected climatic variations in South Carolina [EPA Report, 1998], and the southern and eastern coastal areas of North America in general will have unknown, but potentially significant effects on coastal ocean biogeochemical cycling.

The intertidal zone is transitional between subaerial and shallow submarine conditions, and field observations document the effects of low tide rainfall as a sediment redistribution process. For example, rainfall-enhanced intertidal sediment transport may intermittently control suspended sediment concentrations observed in marsh channels [e.g., Ward, 1981], giving rise to a salt marsh rather than terrestrial geochemical signature [e.g., Gardner, 1975]. Rainfall intensity as low as 11 mm/hr (based on 15 min averages) can increase suspended sediment concentration in tidal creeks from 10 mg/l to approximately 50 mg/l [Voulgaris and Meyers, 2004]. High intensity thunderstorms, common events in tropical and subtropical coastal areas, provide rainfall with greater kinetic energy and produce substantial increases of 100-1000 times above background suspended sediment concentration [Settlemeyer and Gardner, 1975]. Mwamba and Torres [2002], using a portable sprinkler system, estimated that a single thunderstorm may entrain as much as 67-120 tons of marsh sediment per km^2; they reasoned that rainfall effects break apart the low tide sedimentary surface and thereby facilitate transport of the typically cohesive sediment.

Benthic microalgal assemblages inhabiting intertidal and shallow subtidal sediments in many estuaries consist primarily (~90%) of motile and non-motile diatoms [Pearse, 1977]. Euglenoids, green algae and cyanobacteria may also be present, and extensive cyanobacterial mat formation may occur. These benthic microalgae and their products represent nutritious particulate matter [Decho, 1988; 1990; Kneib et al., 1980; Peterson and Howarth, 1987; Robertson et al., 1981; Sullivan and Moncreiff, 1990], and therefore are important participants in nutrient cycles [Hopner and Wonneberger, 1985; Rizzo, 1990]. Additionally, these benthic microalgal assemblages help stabilize soft sediments [Delgado et al., 1991; Holland et al., 1974; Paterson et al., 1990].

Enhanced sediment stabilization occurs through binding of sediment particles with exopolymers which are copiously produced by motile benthic diatoms [Decho, 1990; Frankel and Mead, 1973; Holland et al., 1974; Paterson 1989]. Motile benthic diatoms are capable of rapid movement (1-25 $\mu m\ s^{-1}$) throughout the upper few millimeters of sediment [Edgar and Pickett-Heaps, 1984; Pinckney et al., 1994; Round, 1971]. In southeastern salt marsh sediments, ~33% of the total benthic microalgal biomass is in the upper 1 mm, but migration is detectable to depths of at least 5 mm [Pinckney et al., 1994]. This diatom mobility results in the distribution of exopolymers, leading to greater cohesion and most likely, higher critical shear stress. Subsequent sediment dehydration during low tides enhances biogenic cohesion by thickening the matrix, resulting in increased sediment biostabilization [Paterson et al., 1990]. Low tide rainfall events may substantially disrupt the microbial exopolymer-sediment matrix, with subsequent transport of matrix aggregates toward tidal creek networks, and delivery to the subtidal zone. Hence, low tide rainfall-runoff processes could greatly impact benthic microalgal assemblages during midday low tides when most of the diatom biomass is concentrated in the upper 1 mm of sediment [Pinckney et al., 1994]. Low tide rainfall may also offset desiccation effects, and rainfall percussion can lead to increased diatom mobility [Pinckney et al., 1997].

Rainfall effects may also alter recruitment patterns of microbenthos by changing sediment cohesive properties, exposing subsurface layers, and reducing surficial food quality.

However, these disturbances are expected to have quite different recovery times ranging from hours to days. Increased exposure of subsurface layers, for example, is known to reduce recruitment by a variety of benthic macrofauna, but the surface layer becomes acceptable to recruits within hours, unless disturbed again. Therefore, after repeated disruption (e.g., by resident infauna) do surfaces remain unacceptable [Woodin et al., 1995; Woodin et al., 1998; Marinelli and Woodin, 2002].

Intertidal zone rainfall also affects carbon cycling and sequestration. For example, Oertel [1976] measured increases in suspended sediment and organic matter concentrations during spring tides and rainstorms, and found that the dissolved organic matter (DOM) fraction had a marsh rather than terrestrial source. Therefore, the material entrained during rainfall events may differ compositionally from the bulk average sediment substrate and have different nutritional quality. Oertel reasoned that rainfall-erosion in the marsh produced moderate increases in organic matter (OM) content. Chalmers et al. [1985] measured a net export of organic carbon from a salt marsh during low tide rainstorms. They proposed that rainstorm erosion was a vital process that facilitates carbon cycling in salt marshes, affecting OM accumulation and transformation. Also, Dame and Kenny [1986] found that rainfall-induced nutrient redistribution increased primary productivity. Together these observations show that intertidal zone rainfall events affect biogeochemical processes.

Rainfall kinetic energy represents the total energy available to detach and transport soil particulates by the process of rainsplash, e.g., debris entrainment by raindrop impacts. Conceptually, the annual rain splash transport rate from bare soil is expressed by the general equation [DePloey and Possen, 1985]: $q_s = f(KE, R, D, \beta, B)$, where q_s = the net splash transport rate on smooth bare soil ((m^3/m^2)/year), KE = kinetic energy of rainfall ((J/m^2)/year), R = shear resistance of surface particles, D = particle size, β = slope angle from horizontal, and B = rainfall obliquity from the vertical. In the intertidal marsh, the typically low relief indicates that β is a small number (<10°), although local variations in microtopography and relief along channel banks may be large. In practice, drop velocity is expressed as a 3rd order polynomial of drop diameter [Beard, 1976], and kinetic energy is an exponential function of rainfall intensity [Roswell, 1986], expressed in J/m^2.

Hartley and Alonso [1991] numerically simulated the shear stresses of different raindrop sizes falling into water depths of 0-5 mm. They showed that bed shear stresses induced by drop deformation and water replacement range from 0.4-668 Pa ($Pa = N/m^2$), and were inversely related to water depth. Although raindrop shear stresses are short-lived (<1 millisecond, e.g., Ghadiri and Payne, 1981; Huang et al., 1982; Hartley and Alonso, 1991), field studies indicate that they are of sufficient magnitude and duration to initiate soil particle motion. Therefore, low tide rainfall-runoff processes likely augment intertidal zone material cycling.

Houwing [1999] summarized critical shear stress values from various intertidal environments, and reported a range of 0.02-0.70 Pa, and Amos et al. [1998] reported biostabilized mudflat values of <2 Pa, consistent with the findings of Tolhurst et al. [1999]. Estimates of bed shear stress associated with sheet flow over the intertidal zone indicate that tidal flows do not typically exceed the critical shear value [Shi et al., 1996]. Also, Mimura [1993] examined bed shear stresses induced by shallow water waves and showed that 1.4-13.7 cm waves with periods of 0.77-1.3 s generated bed shear stresses that were typically <1 Pa. These studies demonstrate that critical shear stress, and tidal or shallow water wave bed shear stresses are typically <3 Pa in micro- to mesotidal environments. Hence, bed shear stresses induced by rainfall typically exceed the critical shear of intertidal sediments, and greatly exceed the shear stresses associated with ordinary tidal inundation and oscillatory shallow water wave action.

Taken together, these observations and inferences indicate that low tide rainfall on the intertidal landscape likely enhances material cycling by enhancing the availability of dissolved and particulate organic carbon and nutrients, and low tide rainfall may significantly affect the life cycle of intertidal flora and fauna. The purpose of this paper is to describe the intertidal rainfall-induced material transport processes, and to present data and analyses that might shed light on the effects of rainfall on intertidal ecosystem function.

The Process of Rainfall-Induced Material Transport

As the tide ebbs, subtle topographic variations observed in intertidal salt marshes and mudflats control the occurrence of low tide ponding, and the saturation conditions of exposed sediment. For example, surface drainage of higher areas cause the lower elevations to accumulate or transmit salt water runoff long after the ebb tidal wave has passed. Also, capillary retention forces may offset subsurface drainage and surface desiccation due to evapotranspiration. Consequently, low tide rainfall onto a fine textured intertidal environment will likely occur on ponded, or near-saturated to saturated sediment.

Vegetation canopy will tend to offset raindrop impact effects by intercepting some kinetic energy and by reducing drop size and impact velocity; the degree of energy dissipation depends on the density of the vegetative canopy cover. Some vegetation-intercepted water may flow along living or dead leaves and stems, removing particulate matter along the way, and eventually arrive at the ground surface (stem flow). The leaf area index or LAI (the total, one sided leaf area per unit area of ground) is positively correlated with the biomass of the plant canopy and varies with season, and spatially within the marsh [Morris, 1989]. For example, salt marsh biomass is normally higher adjacent to the tidal creeks [Mendelssohn and Morris, 2000]. Annually, LAI in a typical salt marsh varies from about 0.5 to 3.3 [Jensen et al., 2002], and the greatest canopy biomass occurs late in the summer; and the minimum occurs during winter. Also, in southeastern marshes biomass of the dead leaves from the previous growing season will be substantial during winter, somewhat smoothing out the seasonal effects of LAI. Hence, accumulations of expired annual grass, litter layers or peat will absorb rainfall kinetic energy and continue to protect the sedimentary surface from energetic raindrop effects. For example, Hudson [1971] measured sediment yield from a bare plot and one protected by fine mesh wire gauze (100% ground surface protection) and found a two order of magnitude greater response in the bare soil site. Also, ponded water of sufficient depth will absorb raindrop kinetic energy [e.g., Green and Houk, 1980], but there are contradictory results concerning the effect of water depth on momentum dissipation, expressed as particle detachment, e.g., between Ghadiri and Payne [1988] and Palmer [1963].

On the other hand, openings in the canopy of vegetated marsh (e.g., *S. alterniflora*) permit some rainfall to pass through it (throughfall) and directly impact the substrate. Measurements of throughfall, canopy interception and stem flow have not been reported from intertidal environments. In contrast to the vegetated marsh, intertidal mudflats have negligible vegetative cover, and nearly all raindrops directly impact the substrate, converting kinetic energy to work. Consequently, rainfall-driven material cycling should be substantially greater and more frequent for intertidal mudflats.

Numerous studies reported in the geomorphic and agricultural literature have investigated inter-rill erosion, which is essentially the combination of rainfall-driven detachment and sheetflow transport of sediment [see summary by Bryan, 2000]. Each raindrop striking a surface can be thought of as a "point source" of momentum loss per area, per time [e.g. Gabet and Dunne, 2004]. Pressure exerted by the drop is equal to the rate of momentum

loss per area, and equal to the momentum gain by the surface. A soft surface can absorb momentum by consolidation or deformation (e.g., cratering). Also, some of the impact momentum may not be absorbed, but reflected upwards, transporting water and sediment away from the impact site. Numerical results of Huang et al. [1982] report that the highest compressive stresses occur at the point of raindrop impact and at the perimeter of the rebound corona. Ghadiri and Payne [1981] measured maximum compressive stress of 4.4 MPa that were attributed to a local water hammer effect caused by an initial shock wave. Although these results are for a solid horizontal plane, they illustrate the order of magnitude compressive stresses that can be expected from raindrop impacts. Also, if the unconsolidated surface is saturated raindrop percussion may lead to localized overpressuring and liquefaction of the substrate, perhaps facilitating greater sediment entrainment [De Ploey, 1971].

Immediately after impact the raindrop is deformed and the vertical force is transformed to a lateral shearing force by water jetting over the sedimentary surface. Consequently, these fluid shear stresses may be considered an erosive agent, as shown by Hartley and Alonso [1991], with the potential to detach highly cohesive intertidal sediment. Moreover, these shear stresses are typically several orders of magnitude greater than shear stresses that were observed during over-marsh tidal flows [e.g., Christiansen et al., 2000]. Hence, more raindrops entrain more sediment, with net transport occurring in a direction determined by rainfall obliquity or topography. Field observations support the view that rainfall-driven entrainment and transport processes occur in the intertidal zone and these processes redistribute substantially more sediment than ordinary tidal flows [Mwamba and Torres, 2002].

Since the intertidal surface sediments may be at or near saturation very little rainwater goes into subsurface storage. Therefore, direct precipitation and stem flow lead to runoff development shortly after the inception of rainfall. Freshwater flowing over the surface and freshwater accumulations in intertidal zone depressions are likely to alter the pore water chemistry of the upper few millimeters of intertidal sediments, resulting in a freshwater disturbance to marine microorganisms. Likewise, topographic depressions may be sites of sediment accumulation. After freshwater fills most of the topographic depressions, a more continuous sheetflow develops, facilitating greater material transport in the downslope direction. Also, the sheetflow may absorb some of the incident rainfall kinetic energy and offset sediment detachment, but rain-induced turbulence can help keep mobile sediment particles in suspension while undergoing advection and eventual delivery to tidal creeks. Hence, rain falling onto sheetflow facilitates the transport of sediment over larger distances. Energetic rainfall and sheetflow result in the delivery of sediment-laden water to low order tidal creek networks, eventually reaching subtidal channels. Hence, the magnitude of rainfall intensity and duration will affect the delivery of material to the subtidal channels. Once in the subtidal zone, the fate of rainfall-mobilized material remains unresolved. Does the material settle in the subtidal zone? Does it settle onto the marsh with subsequent marsh inundations? Or, is the material exported to the coastal ocean? Although the fate of this material is not exactly known, low tide rainfall-driven material transport represents a component of biogeochemical *cycling* that has received very little attention. Thus, rainfall-driven sediment transport reintroduces intertidal sediment to the water column from a potentially significant store of carbon and nutrients, and possibly contaminants. Rainfall erosion may augment cycling of the dissolved load as well.

Morris [1995] argued that diffusive exchanges of solutes during marsh inundation are small and cannot account for observed changes in pore water solute concentrations. Consequently, tidal creeks cannot be a source of soluble reactive phosphorous or NH_4 because the diffusion gradient is in the opposite direction. Indeed, depth profiles suggest

that nutrient concentrations in the sediment are dominated by regeneration (decay processes) within the root zone, drainage, salt water and rain water infiltration, and mixing with deeper water. Strong seasonal cycles indicate that temperature-dependent decay processes dominate during warm summer months, and water loss from drainage and evapotranspiration is replaced by flood tide water or rainwater, diluting the solutes in surface sediment [Morris, 1995]. Together these observations indicate that low tide rainfall on intertidal sediment may yield a large and high quality source of food and nutrients that otherwise may not be as accessible to higher trophic levels. The exchanges of nutrients at the marsh surface and those due to drainage are unknown.

In addition to material cycling, rainfall may offset sediment desiccation effects, decrease water salinity in creeks and pools, and in pore water, and it may help wash material from standing vegetation. Also, rainfall erosion may affect surface elevations [Meeder, 1987], particularly important around surface elevation tables (SETs) where sub-millimeter accretion/erosion changes are recorded [e.g., Cahoon et al., 2002]. We go on to speculate that rainfall disruption of biostabilized surface sediment may create conditions that favor sediment transport by ordinary tidal and wave currents that, without the rainfall-runoff effects, likely would not occur. Finally, the work done by rainfall-runoff on intertidal sediment has an unknown effect on the development and stability of salt marsh landscapes. For example, Novakowski et al. [2004] recognized that at North Inlet, intertidal creek networks are topologically random, just as with terrestrial networks. This observation leads to the question: To what extent are intertidal landscapes "etched" by low tide rainfall events, giving the apparently similar creek network topology?

Taken together these studies, observations and inferences indicate that low tide rainfall may be an important intertidal zone sediment and nutrient cycling process. Although much work has been done on rainfall and runoff as a mechanism for sediment entrainment and transport in terrestrial landscapes, rainfall-driven sediment transport in the intertidal zone is complicated by: (1) substantial biogenic cohesion, (2) sediments at, or very close to saturation, (3) the bi-directional forces of flood and ebb tides, and (4) periodic, high tide protection of the sedimentary surface.

Study Site

North Inlet, near Georgetown, South Carolina, is in a subtropical region with average monthly temperatures of 9-27 °C, and annual rainfall of 1.4 m (National Climatic Data Center COOPID #383468). The North Inlet estuary is a 32 km^2 bar-built, ebb-dominated, micro to meso tidal (~1.5 m tides) lagoonal type estuary bordered to the south by a broad mud flat, to the east by a Holocene barrier beach system, and to the west by forested relict beach ridges (see also Gardner, this volume). Large tidal channels (~5-200 m wide) dissect the expansive, low relief salt marsh platform, and smaller tidal creeks (0.5-5 m width) etch the marsh platform, becoming "dry" at low tide. In an 8.7 km^2 area of the estuary there are 725 individual, discrete creek networks with total creek length of 114 km, giving an average drainage density of 13.1 km/km^2 [Novakowski et al., 2004].

Detailed RTK-GPS surveys of the subtle marsh platform topography reveal ~0.70 m of total relief, or 2.5 m when including the smaller tidal creeks [Montane and Torres, submitted]. That part of the marsh bordering the forest is on the side slopes of relict beach ridges, but seaward, away from terrestrial effects, the maximum relief results from levees formed on the banks of larger tidal channels. Differences in marsh elevation distinguish high marsh from low marsh, reflected in distribution of vegetation. Seaward, the high marsh vegetation transitions from maritime forest to *Juncus roemerianus* to *Salicornia*

virginica to short-*Spartina alterniflora* to tall-*Spartina alterniflora* in the low marsh. Typically, the channel banks have tall *S. alterniflora*, and short *S. alterniflora* on the levees. The regularly inundated channel is muddy and unvegetated.

Study plots were located at high marsh, low marsh and channel bank sites [see Mwamba and Torres, 2002]. The high marsh plots had short *S. alterniflora* growing on a firm sand surface with dispersed accumulations of <2 mm fecal pellets and 10-15 mm crab burrow openings. The low marsh plots were at the head of a first-order tidal creek, vegetated with tall *S. alterniflora* growing in mud. The creek head is characterized by subtle but well-defined convergent topography with approximately 0.3 m local relief. The channel bank plots were along a straight artificial channel dredged in 1958 [Dennis Allen, pers. comm., 2002]. The channel bank sites had characteristically dense stands of tall *S. alterniflora* growing in mud. The low marsh and high marsh sites had slopes <0.06 but the channel bank surfaces had slopes of approximately 0.25.

Sediment budget studies show that North Inlet is a sediment sink, in that it imports suspended sediment from the Atlantic Ocean and Winyah Bay [Gardner et al., 1989; Vogel et al., 1996]. The inorganic fraction accounts for 80-85% of the accumulating mass [Gardner and Kitchens, 1978; Vogel et al., 1996]. The organic fraction (15-20%) is derived from a variety of sources that include remains of algae, animals, microbes, terrestrial vegetation and marsh plants [Goni and Thomas, 2000], the latter mainly *S. alterniflora*. ^{137}Cs analyses show that local annual average sediment accumulation rates range from 1.3-2.5 mm/yr [Sharma et al., 1987]. This accumulation rate is comparable to the local sea level rise rate of 2.2-3.4 mm/yr; hence, the marsh surface is rising with sea level [Vogel et al., 1996]. Conversely, it has been hypothesized that the North Inlet marsh-estuary system is a source of organic matter for the coastal ocean [Dame et al., 1986].

The high channel density, extensive first order channelization and convergent topography interact to establish a material exchange system connecting the coastal ocean and the highly productive salt marsh ecosystem. The creek networks also facilitate rainfall-driven material cycling from the intertidal marsh to the coastal ocean. In order to gain further insight into low tide rainfall-runoff processes and their effects on marsh, estuarine and coastal ocean ecosystems a more detailed understanding to intertidal zone topography, it's origin and stability, is required. Presently, there are only a few detailed topographic maps of salt marsh environments reported in the literature.

Methods

The goal of this study was to simulate sediment transport driven by high rainfall intensity (~100 mm/hr) thunderstorms, and to evaluate the effects of natural rainfall on turbidity in a larger subtidal creek. Rainfall simulations were conducted on 1×2 m plots located in the high marsh, low marsh and channel bank; experiments were conducted on April 15, May 27 and June 24, 2000, respectively. We sprinkler irrigated with fresh water and salt water to distinguish between the effects of rainfall-runoff from pore water dilution (e.g., fresh water decreases electrostatic cohesion in flocs, salt water would not) on sediment transport. Flood irrigation (experimental equivalent of ebb tide sheetflow) experiments were performed with salt water over 1×3 m plots to simulate ebb tide effects on sediment transport. In each case, plot runoff was collected at 30-second intervals until a quasi-steady state discharge occurred, and thereafter at various intervals. The water-sediment mixture was stored in a cold room set at 2°C and after 2-4 days the mixtures were separated by centrifugation. See Mwamba and Torres [2002] and Torres et al. [2003] for greater experimental detail and additional findings. Here we report analyses on the sediment fraction in the runoff.

Natural rainfall events were monitored with a second tipping bucket rain gage that measures rainfall totals over 15 minute intervals at 0.01 inch increments. The rain gage is located approximately 150 m from the surrounding forest edge, on a pier within the marsh. A turbidity meter using optical backscatter technology (OBS 3, D&A Instruments) is installed in the middle of a tidal creek at the end of the pier, near the rain gage, with the sensor approximately 0.5 m above the channel bed. Two-minute averaged turbidity values were recorded every 30 minutes in nephelometric turbidity units (NTU). A second rain gage was installed in late April, 2003, approximately 3.2 km to the southeast of the rain gage-station, and it was set to record rainfall at 1-minute (and later 2 minute) intervals.

Nitrogen and Carbon Elemental Analysis

We measured weight percent of organic carbon (%OC) and nitrogen (%N) using the procedure of Hedges and Stern [1984]. Briefly, oven-dried sediment samples were homogenized and weighed (2-5 mg) in silver boats, placed in a vacuum desiccator and then vapor acidified for 24 hours to remove inorganic carbon. The silver boats were inserted into tin boats, folded, and loaded into a Carlo Erba NC 2400 elemental analyzer for organic carbon (OC) and total nitrogen (N) analyses. The samples were analyzed using a combustion temperature of 1020 °C and reduction temperature of 640 °C. Replicate analyses of the same sample resulted in analytical errors of ±2% of the measured value for OC and N.

The stable isotopic compositions of organic carbon ($\delta^{13}C_{OC}$) were determined for pre-acidified samples using automated on-line combustion followed by conventional isotope ratio mass-spectrometry [e.g., Fry et al., 1992]. Analyses were performed using a Finnigan Delta XL-Plus isotope ratio mass spectrometer linked to a Carlo Erba NC 2400 elemental analyzer. Combustion conditions were identical to those used for elemental analyses. By convention, the $^{13}C/^{12}C$ ratio of the organic carbon in any sample is reported in the usual $\delta^{13}C$ parts per thousand, or per mil (‰) notation relative to the international PDB (Pee Dee Belemnite) standard. Based on replicate analyses, the typical analytical error for these types of samples is ±0.3‰.

Atomic N:C ratios were calculated from the OC and N weight percent data. We have chosen to report ratios of N/C rather than C/N because the former are more robust statistically, since the higher number (%OC) is in the denominator, and N/C ratios behave linearly in end member mixtures [Hedges et al., 1986; Jasper and Gagosian, 1990; Keil et al., 1994; Gordon and Goñi, 2003]. Furthermore, by normalizing the N content to the C content of each sample, we keep consistency with the $^{13}C/^{12}C$ data, which in essence are also carbon-normalized.

Results and Discussion

Comparing sediment in runoff from the high marsh (HM), low marsh (LM) and channel bank (CB) plots shows that the HM sprinkler experiment sediment yields, and all flood irrigation (FL) sediment yields were 0.15-4.5% of the sediment yields from the LM and CB plots. Hence, the HM and FL sites and treatments produced negligible amounts of sediment relative to the LM and CB sites (in most cases sample sizes were too small for further analyses). The low HM fluxes most likely resulted from a much lower sheetflow depth (and discharge) due to greater infiltration rates (e.g., transport limited) of the coarser and denser sand substrate and low topographic gradients. For the FL experiments we infer that the low sediment yield results from the absence of rainsplash detachment and raindrop

shear stresses. As a consequence of these findings, hereafter, we focus on the LM and CB sprinkler irrigation experiments. Rainfall intensities for these experiments range from 99-107 mm/hr.

Material entrained by rainfall-runoff had a factor of ~10 difference in weight percent organic carbon (%OC), nitrogen (%N) and inorganic carbon (%IC), in decreasing order, respectively (Figure 2). Also, all of these values are elevated relative to the substrate by a factor ~10 (substrate: %OC ~1.0, %N~0.2, %IC< 0.001), enriched by rainfall-runoff fractionation of the substrate [Torres et al. 2003]. The %OC and %N values from LM-freshwater irrigation (LMFW) and LM-salt water irrigation (LMSW) sites were greater than the LM-flood irrigation (LMFL), and CB-fresh water (CBFW) and CB-salt water (CBSW) results. Also, the CBSW %OC and N data were slightly elevated relative to CBFW, but after ~20 minutes their respective differences were not clearly defined.

Organic Carbon Response

A time series of %OC in samples taken during the LMFW and LMSW irrigations show a nearly uniform to slightly declining response, with means of $7.63 \pm 0.19\%$, and $7.13 \pm 0.57\%$, respectively (Figure 2). The results from a student t-test ($\alpha = 0.05$) show that the means are not significantly different. On the other hand, the LMFL response shows a sharper decline in weight percent with time, as do the CBFW and CBSW responses, and these rates of decline are similar. After approximately 40 minutes, however, the concentration of POC in the remaining two samples (at 47-60 minutes) was similar, indicating an arrest of the declining trend. Therefore, at the LM site, rainfall-runoff processes tend to entrain material of uniform %OC content but the FL treatment, which does not include rainfall impacts, shows a gradual decline. At the more steeply sloping CB sites the rainfall treatment produces a similar response to the LMFL, a decreasing %OC trend.

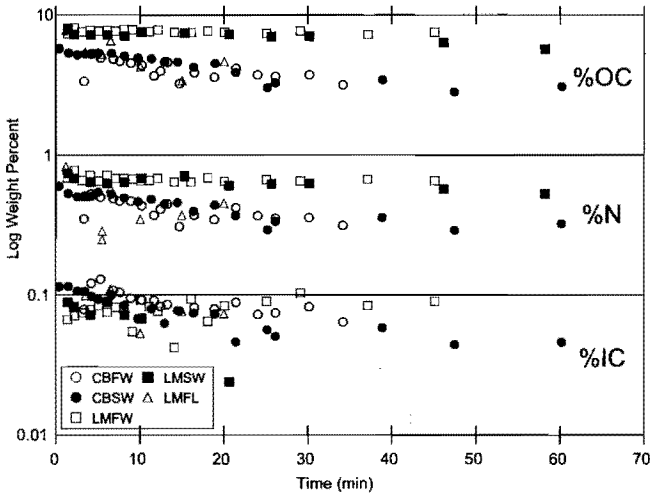

Figure 2. Time series of %OC, %N and %IC from the low marsh (LM) and channel bank (CB) sites irrigated with fresh water (FW) and salt water (SW). Small sample sizes from flood irrigation (FL) treatments precluded a greater number of analyses.

Nitrogen Response

The %N time series for each treatment and location are similar to the %OC response. A time series of %N in samples taken during the LMFW and LMSW irrigations are nearly uniform, with means of $0.67 \pm 0.032\%$, and $0.64 \pm 0.059\%$, respectively (Figure 2). Student t-tests ($\alpha = 0.05$) show that these means are not significantly different. Alternatively, as with the %OC response, the %N time series of the other sites and treatments depict a clear declining trend. For example, the CBFW and CBSW time series show a steadily decline, and the LMFL irrigations depict a highly variable, but declining trend.

Organic Carbon vs. Nitrogen

The %N values range from 0.28-0.85%, and the %OC values range from 2.7-8.1%, indicating an approximate factor of 10 difference between them (Figure 3). The measured N and OC contents for all samples analyzed show a strong linear correlation ($R^2 = 0.93$), with the correlation function having a slight positive x-intercept (Figure 3) for zero %OC. This result is consistent with the presence of a small fraction of inorganic nitrogen (likely ammonia) in these acid-treated samples that is not associated with organic matter [Hedges et al., 1986]. Overall, results from fitting a least squares linear correlation function through all of the data indicates that elevated %OC and %N contents and N:C ratios relative to the substrate are the result of preferential transport of N-rich organic matter with some component of inorganic N [see Torres et al., 2003].

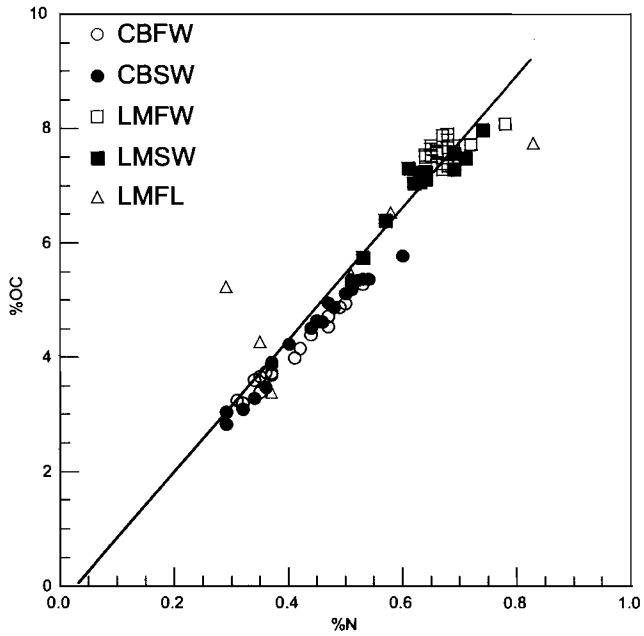

Figure 3. Plot of %OC vs. %N data from all sites, with all treatments showing a slight negative y-intercept. Note the separation between CB and LM data.

On the other hand, a different interpretation emerges when considering linear trends through the same data, but separated by location and treatment. First, the LM data plot furthest up the curve fit, indicating that LM samples have the highest %OC and %N. The CB data plot closer to the origin, indicating less enrichment. We speculate that enrichment of rainfall-mobilized sediment increases away from the channel and that similar %OC-%N data from suspended sediment in the channel will likely plot along the trend line in Figure 3, between the origin and start of the CB data.

Atomic N/C ratios for CB treatments are slightly higher than both samples from LM sites but they are not significantly different ($\alpha = 0.05$), consistent with our findings described above (Figure 4). On the other hand, the CB sample means are significantly ($\alpha = 0.05$) more depleted in ^{13}C. These isotopic data indicate that the OC in samples is from a mixture of C3 and C4 plants, with the dominant plants being *J. romerianus* and *S. alterniflora*, respectively. Plotting the N/C values against $\delta C^{13}{}_{OC}$ indicate that both the CB and LM samples are enriched in organic matter originating from marine algae, which may include benthic diatoms. Hence, the high nutritional quality of these sediments results, in part, from the rainfall controlled entrainment of algal derived organic matter.

A time series of 12-20 samples analyzed for $\delta^{13}C_{OC}$ for each location and treatment depict some variability but do not reveal any particular trend. LMFW values range from −18.8 to 18.3‰ with a mean of 18.6 ± 0.14‰, while LMSW values range from −18.8 to −18.4‰ with a mean of -18.7 ± 0.10‰. These values are not significantly different

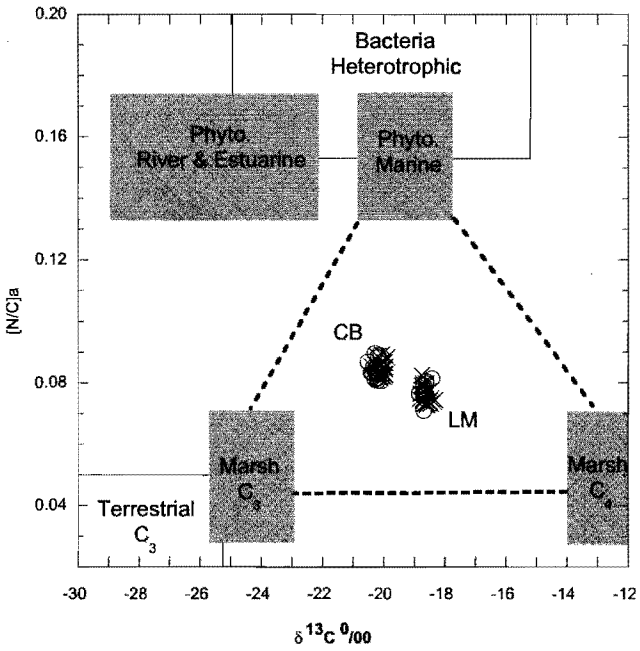

Figure 4. Atomic N/C ratios vs. δC^{13}‰ showing that the sediment entrained by rainfall has a mixture of C3 and C4 plants, and marine microalgae. CB denotes the channel bank cluster of data and LM denotes the low marsh. Cross symbols depict fresh water data and open symbols depict saltwater data. Shaded and open rectangles identify the range of values for various carbon sources.

($\alpha = 0.05$). CBFW samples range from –20.4 to 19.9‰ with a mean of 20.1 ± 0.12‰, while CBSW values range from –20.5 to –20.0‰ with a mean of -20.2 ± 0.12‰. As with the LM data, these CB carbon isotope data are not significantly different ($\alpha = 0.05$). On the other hand, the LM values are significantly different from the CB data ($\alpha = 0.05$).

Inorganic Carbon Response

The %IC time series is distinct from %OC and %N responses (Figure 3). The LMFW data show an increase for the first six minutes, and thereafter a highly variable increasing trend continues, albeit at a much lower rate. Conversely, the LMSW irrigation produced a response in %IC with the greatest rate of change, from 0.09% to 0.02% over the first 21 minutes. The CBSW data show a more gradual and steady decline from 0.11% to 0.045% over the first 22 minutes, after which the values are variable and without a clear trend, fluctuating between 0.04% to 0.06%. The CBFW data increase to 0.13% over the first five minutes and are typically ~0.02% greater than the CBSW data. The LMFL data also show a decrease with time.

The %IC responses from the LMFW and CBFW show an increase over the first few minutes of irrigation before settling to within some quasi-steady range of values. Nevertheless, we interpret the initial increase in %IC as resulting from a freshwater (rainfall) disturbance to the surface sediments, promoting activity in inorganic carbon-bearing microfauna, and subsequent transport by rainfall-runoff. Although the data points are few, the increases over the first few minutes are clearly illustrated.

Effects of Rainfall Mobilization

Overall, our results show that low tide rainfall events may entrain nutritious particulate matter from both the channel banks and the low marsh. The declining response of %OC and %N at the CB sites, however, suggests that CB nutrients have a more limited abundance relative to the LM. For example, the nearly uniform responses of %OC and %N during low marsh irrigations indicates that, at least for the duration of these experiments, low tide rainfall may entrain more nutrients per unit area. Moreover, the total area of low marsh is approximately three orders of magnitude greater than the channel bank area.

Using cumulative flux (kg) from a known area (m^2) and bulk density (kg/m^3), all reported by Mwamba and Torres [2002], we estimate that during the first 10 minutes of irrigation, approximately 0.2 mm of surface sediment was "exported" from the LM plots, or 8-15% of the local annual average accumulation of 1.3-2.5 mm/yr determined using ^{137}Cs as a stratigraphic marker [Sharma et al., 1987]. Scaling-up the plot rainfall simulation results to the North Inlet marsh platform area of ~25 km^2 (excluding 7 km^2 of water) gives order of magnitude approximations for sediment yield per storm. The LM and CB areas together produce 67-120 tons of material per km^2 with 10% OC content [Torres et al., 2003] per 10-minute storm. Therefore, approximately 7-12 tons/km^2 of organic carbon may be mobilized during this time. Of course, not all sediment mobilized by rainfall becomes available for broader redistribution.

We hypothesize that sheetflow velocity and duration control the delivery of sediment to the intertidal creeks, and once there higher energy flows controlled by the channel gradient facilitate delivery to subtidal creek and possibly broader redistribution. For example, each minute of rainfall duration leads to a progressively larger swath of marsh delivering sediment-laden rainwater directly to the creek network. Given an intertidal creek density of 13.1 km/km^2 [Novakowski et al., 2004], and given an average sheet flow velocity of

2 cm/sec [Mwamba and Torres, 2002], and using estimates of OC mobilization derived from plot experiments [Torres et al., 2003], we infer that a 10-minute long, low tide, high intensity rainstorm (~100 mm/hr) delivers 34-60 tons of particulate OC (POC) to intertidal creeks. Moreover, once in the water column the recycled material may be subject to degradation or enrichment processes. At North Inlet, between mid-July to September 2003 there were six low tide thunderstorms, and if our order of magnitude approximations are correct then 202-362 tons of POC may have been delivered directly to the tidal creek system. This corresponds to 16-31% net summer export of POC to the coastal ocean [for POC budget see Dame et al., 1986]. Of course, not all of this material is exported but clearly rainfall events increase availability of material for possible export. Based on these estimates, it appears that low tide summer storms may have a significant, but as yet largely unrecognized impact on estuarine material cycling. In particular, low tide rainfall-driven material fluxes represent a potentially important "non-point source" of carbon and nutrients to the ecosystem. Additionally, rainfall-runoff processes may recycle contaminants adsorbed to intertidal sediments.

Clearly, these estimates of rainfall-induced material flux are order of magnitude approximations and should not be construed as definitive of the location or process; much work remains. For example, we have not explored the relationships between rainfall intensity, duration and frequency on sediment yields. We did not account for temporal and spatially variable canopy cover or the seasonal activity of benthic fauna, and the indirect effects of rainfall are not known. Also, rainfall disruption of a biocohesive surface layer may cause subsequent tidal and wave resuspension of intertidal sediments that otherwise may not have occurred, and the fate of this rainfall-entrained material is unknown. Intuitively, one possible fate is its redeposition onto the marsh surface within the next few tidal cycles. Alternatively, this material may be exported from the estuary to the coastal ocean. We speculate that the actual fate of rainfall-entrained intertidal sediment may be some combination of these end member cases.

Irrespective of the exact amount of material entrained by low tide rainfall, and its ultimate fate, we hypothesize that the entrainment of sediment and associated organic matter from the intertidal zone during low tide rainfall events has a poorly understood role in the overall carbon and nutrient cycles of coastal systems, and this material has been largely unaccounted for due to the stochastic nature of the process and the difficulty of studying these short-term events. Consequently, several key questions regarding low tide rainfall-driven material cycling persist:

- How frequently do low tide rainfall events occur?
- Do salt marsh topographic variations facilitate or inhibit wider distribution of rainfall-entrained material?
- How much material is reintroduced to the subtidal water column by low tide rainfall?
- Do similar low tide rainstorms produce a similar turbidity response?
- What is the fate of rainfall-entrained intertidal zone material?

One relatively simple effort that could provide greater insight on intertidal rainfall erosion processes is to have coastal meteorological stations record rainfall totals at 1-2 minute intervals where rain storms are a recurring component of the ecosystem.

Observations During Natural Storms

On May 1, 2003 the North Inlet-Winyah Bay National Estuarine Research Reserve (NERR) began acquiring 15-minute rainfall totals (switching from daily) with a tipping bucket gage, complimenting their long-term data acquisition and archiving

efforts that include turbidity and tidal stage collected at half hour intervals. The 15-minute rainfall totals range from 0.25-19 mm, with 5 events that exceeded 10 mm, and 14 that were between 5 and 10 mm. The remaining 53 storms had less than 4 mm. Turbidity data show diurnal fluctuations that are out of phase with tidal oscillations and range from 4-120 NTU. When rainfall occurs turbidities may increase, in some cases as high as 920 NTU but they usually return to background levels within a few tidal cycles.

We combined the turbidity, rainfall and tidal stage data sets for the interval May 20 – June 19, 2003, days 140-170, shown in Figures 5A and 5B (after day 170.5 the entire instrument package was disassembled for maintenance). This interval was chosen for closer scrutiny because several rainfall events and different types of turbidity response occur. There are 12 discrete rainfall events, identified as periods of continuous rainfall separated by periods of no rainfall, and each rainfall event has one or more short-term maximum rainfall intensities. Turbidity data depict periodic variability associated with tidal fluctuations,

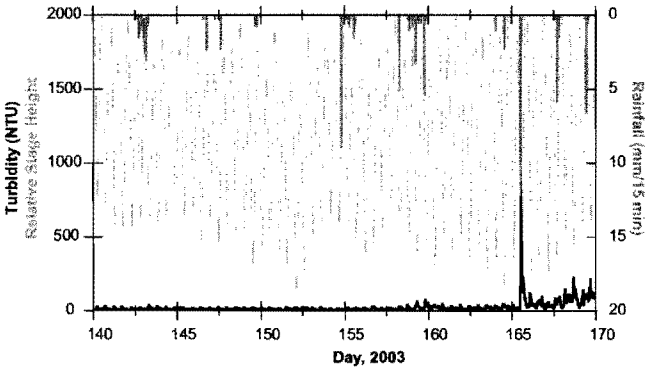

Figure 5A. Time series of turbidity (NTU) on the left axis, rainfall rate (mm/15 min) on the right axis, for a 31-day interval. The tidal stage is shown in gray, as relative values.

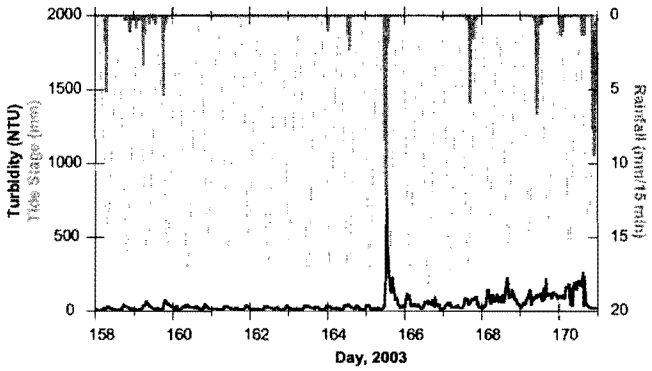

Figure 5B. Time series of turbidity (NTU) on the left axis, rainfall rate (mm/15 min) on the right axis for a 13-day interval shown in Figure 5. The tidal stage is shown in gray, in units of millimeters.

with maximum turbidity values corresponding to low tide. In particular, the turbidity data show that prior to day 158, values range from 4-40 NTU with a mean of 13.4 ± 5.3 NTU. Also, before day 158 five rainfall events occurred but they seem not have affected turbidity readings as no corresponding turbidity change was detected. Closer inspection of these five rain events shows that some rainfall occurred at low tide, but the highest intensity of each event coincided with mid to high tide intervals. Consequently, the sediment surface was protected from rainfall impacts of the highest storm intensities, and the energy associated with lower intensities during low tide were less able to entrain the intertidal substrate.

From day 158-160 two rainstorms occurred with three distinct higher intensity peaks, and three corresponding peaks in turbidity. The event at 158.3 occurred at dead low tide but the corresponding peak at 24 NTU was not much higher than ambient readings. Hence, this first event, although occurring at low tide, did not have a significant impact on sediment entrainment; the peak NTU value for the subsequent low tide interval was slightly higher at 31 NTU. The next rainfall event of day 159.2 occurred midway from high to low tide, and within three hours it was followed by a peak turbidity of 65 NTU. The third high intensity interval at day 159.8 occurred two hours prior to low tide and produced a peak of 76 NTU. Thereafter, the turbidity values remained between 5-30 NTU until day 165.5, despite having two low tide, low intensity, rainfall events.

At about midday on June 14, 2003 a typical summer thunderstorm with subsequent showers occurred over the North Inlet estuary, delivering 38 mm of rainfall in 2.1 hours. Maximum rainfall intensities for this event, however, estimated from a tipping bucket rain gage 2.6 km southeast of the North Inlet-Winyah Bay NERR instrument package was 174 mm/hr for 4 minutes (Figure 1). This thunderstorm occurred just prior to low tide at day 165.5. The work done on sediment by this high-energy event is apparent in the peak turbidity reading of 920 NTU within one hour of the onset of rain. Hence, this rainstorm produced a 20-200 fold increase in turbidity that lasted for approximately 30 minutes, but by day 166 the turbidity reading declined to 28 NTU. Between days 166-170.5 two more rainfall events occurred, with maximum two-minute intensities of 96 and 112 mm/hr respectively, comparable to the sprinkler irrigation intensities. The latter storm was at high tide, while the first, at 167.6 days, occurred immediately after low tide, and while a significant proportion of the salt marsh was still exposed. However, there was no response in turbidity comparable to the storm at 165.5 days. Nevertheless, the turbidity following the day 165.5 storm remained elevated relative to previous readings. For example the average over the 166-170.5 days was 77.3 ± 45.2 NTU. Hence, the average post storm turbidity was nearly double the turbidity detected prior to day 158, where no rainfall effects were observed.

Figure 6 is a polar plot showing the occurrence of all recorded rainfall events of a particular intensity, and the corresponding magnitude of the turbidity response within in the context of a diurnal tidal cycle (12.4 hours). The data show that 15-minute rainfall totals range from 0.25-19 mm, 5 events exceeded 10 mm, and 14 were between 5 and 10 mm. The remaining 53 storms had less than 4 mm per 15-minute interval. Figure 6 also shows that rainfall events occurred at different tidal stages, with 34 of 72 over the "low tide" interval, e.g., they plot on the right half of the polar plot. In combining the rainfall-turbidity response it is clear that all but one of the maximum turbidity values occur as the tide transitions from high to low. In particular, most of the larger responses are shown to occur sometime shortly after high tide to slack low tide. These rainfall-turbidity data and analyses show that moderate to high intensity, low tide rainfall events have the energy to entrain local intertidal material. However, the fate of the material appears to be dependent on the timing of the rainstorm in relation to the tidal phase.

The combination of rainfall events at days 165.5 and 167.6 reveals some details of the fate of rainfall-entrained sediment. Figure 5A shows that the day 165.5 event produced a

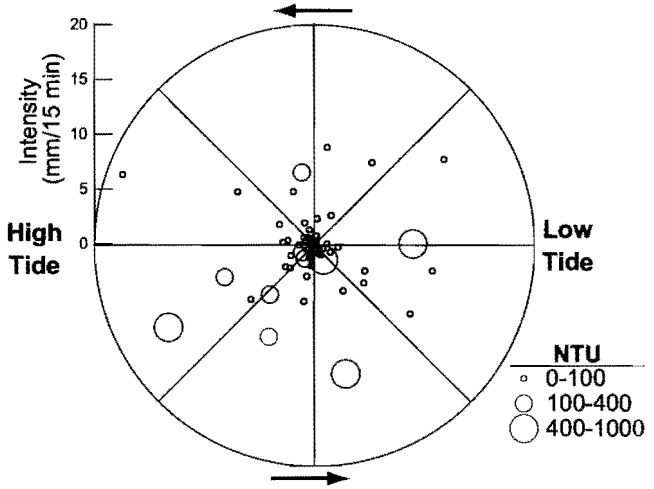

Figure 6. Polar plot of rainfall intensity and tidal stage (relative), with turbidity (NTU); the full circle represents one complete tidal cycle. The length of the line from the plot center to an open symbol depicts rainfall intensity. Projecting a line from the center, through a point and to the polar axis depicts tidal stage for that rainfall event. Different sized symbols represent a classification of maximum turbidity values detected within 12.4 hours of a corresponding rainfall event, small symbol, 0-100 NTU, medium symbol, 100-400 NTU, large symbol, 400-1000 NTU. Arrows depict direction of tidal fluctuations.

large turbidity response, but the low tide storm of day 167.6 did not. This observation indicates that the earlier event entrained most of the mobile material, leaving very little for the latter storm. Hence, over the 2.1 day interval between storms little of the material entrained by the first storm was locally redeposited with the subsequent high tides, and therefore less material was available for transport by the latter rainfall event. This interpretation implies that the rainfall-entrained material may have remained in suspension long enough to be exported from the local area.

The occurrence of both storms relative to tidal stage reveals the role of tidal hydrodynamics on rainfall-induced turbidity changes. Figure 7 shows how tidal stage and current velocity vary throughout the tidal cycle both for neap (dashed lines) and spring (solid lines) tides, respectively, over a period of 15 tidal cycles [Voulgaris and Meyers, in press]. Note that maximum ebb flows occur $\pi/3$ of a tidal cycle (i.e. 2.1 hours) prior to low water. This is due to the frictional effects that create a phase lag between sea surface elevation and current. At times immediately following low water the flow direction switches to flood. This implies that material mobilized by rainstorms occurring after low water (such as the event of day 167.6) is likely to be transported back onto the marsh surface but ebb tide advection may facilitate transport of rainfall-mobilized material to the subtidal system (where our turbidity sensor is located). These observations lead us to infer that there are optimal tidal hydrodynamic conditions that will favor broader material redistribution. For example, under an ebb tide, when the tidal stage is below the "mean tidal stage" (i.e., extensive exposure of intertidal marsh) low tide rainfall-entrained material entering the subtidal system will have the greatest potential to be more widely redistributed. These optimal conditions occur only for approximately 2.6 hours preceding low tide (shown as

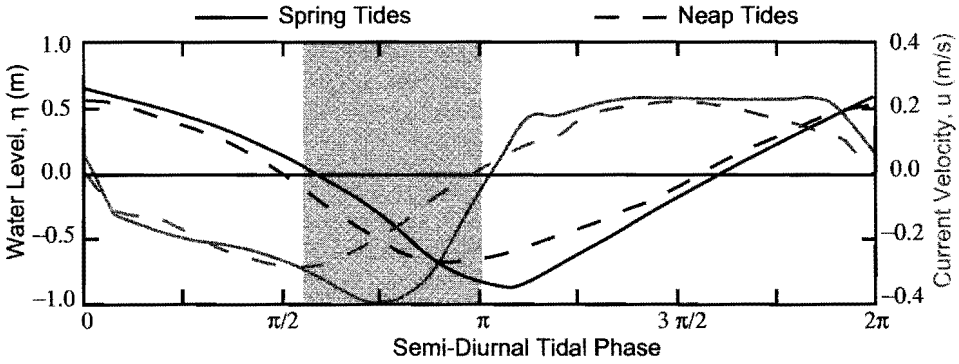

Figure 7. Tidal variability of mean water surface elevation (η) and currect velocity (u) in a tidal creek in North Inlet, SC for spring (solid line) and neap (dashed line) tidal conditions. Shaded area indicates period within a tidal cycle that rainfall–mobilized material is likely to be introduced to the subtidal creek network system and possibly exported. During the remainder of the tidal cycle the marsh is either covered by water or the rainfall-mobilized material is prohibited from entering the creek network because of the flood advection.

shaded area in Figure 7). Hence, rainfall events occurring on an ebb tide may lead to the export of nutritious particulate matter from the marsh, to the estuary and to the coastal ocean, thereby affecting coastal ocean ecosystem function and biogeochemical cycling. This timing between rainfall and tides may account for disparity in turbidity signals reported here. Alternatively, the large turbidity response of the former and slight response of the latter storm indicates that a rainfall intensity threshold to intertidal sediment entrainment may exist, or perhaps there is a non-linear relationship between kinetic energy of rainfall and sediment detachment. Clearly, more research is needed to investigate processes of low tide rainfall entrainment and resulting fluxes, the role of salt marsh topography in material cycling, and the fate of that material once entrained.

Conclusions

Results show that forces associated with raindrop impacts, shear stresses from raindrop deformation and freshwater sheetflow facilitate the cycling of intertidal material that is enriched in organic nitrogen with a mixture of C3 and C4 organic carbon, and algal matter. Also, the degree of N enrichment varies with distance away from the tidal creek. The simulated rainstorm-driven material fluxes indicate that a single thunderstorm may erode 8-15% of annual average sediment accumulation, with POC fluxes equal to 6-10% of the annual POC export or 22-40% of the net summer export from the estuary. Hence, rainfall-entrained intertidal sediment represents a potentially significant "non-point source" of highly nutritious particulate matter. These observations support our contention that rainfall facilitates estuarine material cycling.

The broader redistribution of this nutritious material, however, remains unresolved. Insight gleaned from combined turbidity and hydrodynamic data indicate that for each tidal cycle a 2.4 hour window of tidal hydrodynamic conditions may exist that optimizes the likelihood of estuary wide redistribution or export. Rainfall events at lower intensity or at less than optimal times will yield negligible sediment entrainment, or lead to local

redeposition. Irrespective of the post-rainfall fate of the mobilized material, clearly, intertidal rainfall events facilitate cycling of highly nutritious particulate material. More research should be conducted to ascertain 1) the frequency of low tide rainfall events, 2) the fraction of rainfall-entrained sediment that is susceptible to export to the coastal ocean, and 3) the role of salt marsh topography in rainfall-entrained material cycling.

Acknowledgements. This research was supported by National Science Foundation Grant Number: EAR 9985345 awarded to Raymond Torres. The Winyah Bay-North Inlet NERR supplied rainfall, tide and turbidity data. Mwasi J. Mwamba collected and prepared samples and Karyn I. Novakowski prepared figures and copy edited the final manuscript. Comments from two anonymous reviewers helped improve brevity and clarity of this paper.

References

Admiraal, W., H. Peletier, and H. Zomer, Observations and experiments on population dynamics of epipelic diatoms from an estuarine mudflat, *Estuarine, Coastal and Shelf Science, 14*, 471-487, 1982.

Aleem, A., The diatom community inhabiting the mud-flats at Whitstable, *New Phycol., 49*, 174-188, 1950.

Amos, C. L., M. Brylinski, T. F. Sutherland, D. O'Brian, S. Lee, and A. Cramp, The stability of a mudflat in the Humber Estuary, South Yorkshire, UK, in *Sedimentary Processes in the Intertidal Zone*, edited by Black K. S., Patterson, D. M., and A. Cramp, Geological Society of London, Special Publication 139, 25-43, 1998.

Beard, K.V., Terminal velocity and shape of cloud and precipitation drops aloft, *J of Atm Sciences, 33*, 851-864, 1976.

Bryan, R.B., Soil erodability and processes of water erosion on hillslopes, *Geomorphology, 32*, 385-415, 2000.

Cahoon, D. R., J. C. Lynch, B. C. Perez, B. Segura, R. Holland, C. Stelly, G. Stephenson, and P. Hensel, A device for high precision measurement of wetland sediment elevation: II. The rod surface elevation table. *J. Sed.Res., 72*(5), 734-739, 2002.

Chalmers, A. G., R. G. Wiegert, and P. L. Wolf, Carbon balance in a salt marsh: Interactions of diffusive export, tidal deposition and rainfall-caused erosion, *Estuarine, Coastal and Shelf Science, 21*, 757-771, 1985.

Christiansen, T., P. L. Wiberg, and T. G. Milligan, Flow and sediment transport on a tidal salt marsh surface, *Estuarine, Coastal and Shelf Science, 50*, 315-331, 2000.

Dame, R.F. and P. Kenny, Nutrient processing and the development of tidal creek ecosystems, *Marine Chemistry, 43*, 175-183, 1986.

Dame, R., T. Chrzanowski, K. Bildstein, B. Kjerve, H. McKellar, D. Nelson, J. Spurrier, S. Stancyk, H. Stevenson, J. Vernberg, and R. Zingmark, The outwelling hypothesis and North Inlet, South Carolina, *Marine Ecology Progress Series, 33*, 217-229, 1986.

Decho, A., How do harpacticoid grazing rates differ over a tidal cycle? Field verification using chlorophyll-pigment analyses. *Mar. Ecol. Prog. Ser., 45*, 263-270, 1988.

Decho, A., Microbial exopolymer secretions in ocean environments: their role(s) in food webs and marine processes. *Oceanogr. Mar. Biol. Annu. Rev., 28*, 73-153, 1990.

Delgado, M., V. de Jonge, and H. Peletier, Experiments on resuspension of natural microphytobenthos populations. *Mar. Biol., 108*, 321-328, 1991.

De Ploey, J., Liquefaction and rainwater erosion, *Zeithschrift fur Geomorphologie, 15*, 491-496, 1971.

De Ploey J., and J. Poesen,, Aggregate stability, runoff generation and inter-rill erosion, in *Geomorphology and Soils* edited by K. S. Richards, R. R. Arnett, and S. Ellis, and George Allen, Unwin, London, pp. 99-120, 1985.

Edgar, L. and J. Pickett-Heaps, Diatom locomotion, in *Progress in Phycological Research* edited by F. E. Round and D. J. Chapman, pp. 47-88., Biopress, Bristol, 1984.

Environmental Protection Agency, Climate change and South Carolina, Report 236 F97 007w, 4 pp., 1998.

Frankel, L. and D. J. Mead, Mucilaginous matrix of some estuarine sands in Connecticut, *J. Sed. Petrol. 43*, 1090-1095, 1973.

Fry, B., W. Brand, F. J. Mersch, K. Tholke, and R. Garrit, Automated analysis system for coupled $\delta^{13}C$ and $\delta^{15}N$ measurements, *Anal. Chem., 64*, 288-291, 1992.

Gabet, E.J. and T. Dunne, Sediment detachment by rain power, *Water Resources Research*, 39(1), 10.1029/2001WR000656, 2003.

Gardner, L. R., Runoff from an intertidal marsh during tidal exposure – recession curves and chemical characteristics, *Limnology and Oceanography*, *20*(1), 81-89, 1975.

Gardner, L. R., L. Thomas, and D. Nelson, Time series analyses of suspended sediment concentrations at North Inlet, South Carolina, *Estuaries*, *12*, 211-221, 1989.

Gardner, L. R. and W. Kitchens, Sediment and chemical exchanges between salt marshes and coastal waters, in *Transport Processes in Estuarine Environments*, edited by Kjerfve, B., Belle W. Baruch Library in Marine Science, No. 7, University of South Carolina Press, Columbia, 1978.

Ghadiri, H. and D. Payne, Raindrop impact stress, *Journal of Soil Science* (European), *32*, 41-49, 1981.

Ghadiri, H. and D. Payne, The formation and characterization of splash following raindrop impact on soil, *Journal of Soil Science* (European), *39*, 563-575, 1988.

Goñi, M. A. and K. A. Thomas, Sources and transformations of organic matter in surface soils and sediments from a tidal estuary (North Inlet, South Carolina, USA). *Estuaries*, *23*(4), 548-564, 2000.

Gordon, E. S., and M. A. Goñi, Sources and distribution of terrigenous organic matter delivered by the Atchafalaya River to sediments in the northern Gulf of Mexico, *Geochim. Cosmochim. Acta*, *67*, 2359-2375, 2003.

Green, T. and D. Houk, The resuspension of underwater sediment by rain, *Sedimentology*, *27*(5), 607-610, 1980.

Hartley, D. M. and C. V. Alonso, Numerical study of the maximum boundary shear stress induced by raindrop impact, *Water Resources Research*, *27*(8), 1819-1826, 1991.

Heckman, C., The development of vertical migration patterns in the sediments of estuaries as a strategy for algae to resist drift with tidal currents, *Internatl. Rev. ges. Hydrobiol.70*, 151-164, 1985.

Hedges, J. I. and J. H. Stern, Carbon and nitrogen determinations of carbonate-containing solids, *Limnology and Oceanography*, *29*, 657-663, 1984.

Hedges, J. I., W. A. Clark, P. D. Quay, J. E. Richey, A. H. Devol, and U. de M. Santos, Compositions and fluxes of particulate organic matter in the Amazon River, *Limnology and Oceanography*, *31*, 717-738, 1986.

Holland, A. F., R. G. Zingmark, and J. M. Dean, Quantitative evidence concerning the stabilization of sediments by marine benthic diatoms, *Mar. Biol. 27*, 191-196, 1974.

Hopkins, J., A study of the diatoms of the Ouse estuary, Sussex. I. The movement of the mudflat diatoms in response to some chemical and physical changes, *J. Mar. Biol. Assoc.*, U.K. *43*, 653-663, 1963.

Höpner, R. and K. Wonneberger, Examination of the connection between the patchiness of benthic nutrient efflux and epiphytobenthos patchiness on intertidal flats, *Netherlands J. Sea Res.*, *19*, 277-285, 1985.

Houwing, E.-J., Determination of the critical erosion threshold of cohesive sediments on intertidal mudflats along the Dutch Wadden Sea Coast, *Estuarine, Coastal and Shelf Science*, *49*, 545-555, 1999.

Huang, C., J. M. Bradford, and J. H. Cushman, A numerical study of raindrop impact phenomena: The rigid case, *Soil Science Society of America Journal, 46*, 14-19, 1982.

Hudson, N.W., *Soil Conservation*, Batsford Press, London, 320 pp., 1971.

Jasper J. P. and R. B. Gagosian, The sources and deposition of organic matter in the Late Quaternary Pigmy Basin, Gulf of Mexico, *Geochim. Cosmochim. Acta, 54*, 1117-1132, 1990.

Jensen, J. R., G. Olsen, S. R. Schill, D. E. Porter, and J. Morris, Remote sensing of biomass, leaf-area-index, and chlorophyll a and b content in the ACE Basin National Estuarine Research Reserve using sub-meter digital camera imagery, *Geocarto International, 17*(3), 1-10, 2002.

Joint, I., J. Gee, and R. Warwick, Determination of fine-scale vertical distribution of microbes and meiofauna in an intertidal sediment, *Mar. Biol., 72*, 157-164, 1982.

Keil R. G., E. Tsamakis, C. Bor Fuh, J. C. Giddings, and J. I. Hedges, Mineralogical and textural controls on the organic composition of coastal marine sediments: hydrodynamic separation using SPLITT-fractionation, *Geochim. Cosmochim. Acta, 58*, 879-893, 1994.

Kneib, R., A. Stiven, and E. Haines. Stable carbon isotope ratios in *Fundulus heteroclitus* (L.) muscle tissue and gut contents from a North Carolina *Spartina* marsh, *J. Expt. Mar. Biol. Ecol., 46*, 89-98, 1980.

Marinelli, R. L., and S. A. Woodin, Experimental evidence for linkages between infaunal recruitment, disturbance and sediment chemistry, *Limnol. Oceanogr., 47*(1), 221-229, 2002.

Meeder, J., Variable effects of hurricanes on the coast and adjacent marshes: A problem for marsh managers, in N.V., in *Proceedings of the 4th Water Quality and Wetlands Management Conference* edited by Broadtmann, New Orleans, Louisiana, pp. 337-374, 1987.

Mendelssohn, I. A. and J. T. Morris, Ecophysiological controls on the growth of *Spartina alterniflora*, in *Concepts and controversies in tidal marsh ecology* edited by N.P. Weinstein and D.A. Kreeger, Kluwer Academic Publishers, pp. 59-80, 2000.

Mimura, M., Rates of erosion and deposition of cohesive sediments under wave action, in *Nearshore and Estuarine Cohesive Sediment Transport* edited by A. J. Mehta, AGU, Washington, D.C., pp. 247-264, 1993.

Morris, J. T., Modeling light distribution within the canopy of the marsh grass *Spartina alterniflora* as a function of canopy biomass and solar angle, *Agricultural and Forest Meteorology, 46*, 349-361, 1989.

Morris, J. T., The salt and water balance of intertidal sediments: results from North Inlet, South Carolina, *Estuaries 18*, 556-567, 1995.

Mwamba, M. J. and R. Torres, Rainfall effects on marsh sediment redistribution, North Inlet, South Carolina, *Marine Geology, 189*, 267-287, 2002.

Novakowski, K. I., R. Torres, L. R. Gardner, and G. Voulgaris, Geomorphology of intertidal creek networks, *Water Resources Research*, 40(5) W05401 doi 10.1029 2003/WR002722, 2004.

Oertel, G. F., Characteristics of suspended sediments in estuaries and nearshore waters of Georgia, *Southeastern Geology, 18*, 107-118, 1976.

Palmer, J., Tidal rhythms: The clock control of the rhythmic physiology of marine organisms, *Biol. Rev., 48*, 377-418, 1973.

Palmer, J. and F. E. Round, Persistent, vertical-migration rhythms in benthic microflora. VI. The tidal and diurnal nature of the rhythm in the diatom, *Hantzschia virgata. Biol. Bull., 132*, 44-55, 1967.

Palmer, R., The influence of a thin water layer on water drop impact forces, *International Association of Hydrological Scientists Publication, 65*, 141-148, 1963.

Paterson, D. M., Short-term changes in the erodibility of intertidal cohesive sediments related to the migratory behaviour of epipelic diatoms, *Limnol. Oceanogr., 34*, 223-234, 1989.

Paterson, D. M., R. M. Crawford, and C. Little, Subaerial exposure and changes in the stability of intertidal estuarine sediments, *Est. Coast. Shelf Sci., 30*, 541-556, 1990.

Pearse, J., Radiocarbon tracing of migrating benthic diatoms. M.Sc. thesis, University of South Carolina, Columbia, 1977.

Peterson, B. and R. Howarth, Sulfur, carbon, and nitrogen isotopes used to trace organic matter flow in the salt-marsh estuaries of Sapelo Island, Georgia., *Limnol. Oceanogr., 32*, 1195-1213, 1987.

Pinckney, J. and R. Zingmark, Effects of tidal stage and sun angles on intertidal benthic microalgal productivity, *Mar. Ecol. Prog. Ser., 76*, 81-89, 1991.

Pinckney, J., Y. Piceno, and C. R. Lovell, Short-term changes in the vertical distribution of benthic microalgal biomass in intertidal muddy sediments, *Diatom Res., 9*, 143-153, 1994.

Pinckney, J. L., D. G. Millie, B. T. Vinyard, and H. W. Paerl, Environmental controls of phytoplankton bloom dynamics in the Neuse River estuary (North Carolina, USA), *Can. J. Fish. Aquat. Sci., 54*, 2491-2501, 1997.

Rizzo, W., Nutrient exchanges between the water column and a subtidal benthic microalgal community, *Estuaries, 13*, 219-226, 1990.

Robertson, J., J. Fudge, and G. Vermeer, Chemical and live feeding stimulants of the sand fiddler crab, *Uca pugilator* (Bosc.), *J. Expt. Mar. Biol. Ecol., 53*, 47-64, 1981.

Roswell, C. J., Rainfall kinetic energy in eastern Australia, *J of Climate and Applied Meteorology, 25*, 1695-1701, 1986.

Round, R. E., Benthic marine diatoms, *Oceanogr. Mar. Biol. Annu. Rev., 9*, 83-139, 1971.

Settlemeyer, J. L., and L. R. Gardner, Low-tide storm erosion in a salt marsh, *Southeastern Geology, 16*(4), 205-212, 1975.

Shi, Z., J. S. Pethick, F. Burd, F., and B. Murphy, Velocity profiles in a salt marsh canopy, *Geomarine Letters, 16*, 319-323, 1996.

Sharma, P., L. R. Gardner, W. S. Moore, and M. S. Bollinger, Sedimentation and bioturbation in a salt marsh as revealed by 210Pb, 137Cs, 7Be studies, *Limn. Oceangr., 32*(2), 313-326, 1987.

Sullivan, M. and C. Moncreiff, Edaphic algae are an important component of salt marsh food webs: evidence from multiple stable isotope analysis, *Mar. Ecol. Prog. Ser., 62*, 149-159, 1990.

Tolhurst T. J., K. S. Black, S. A. Shayler, S. Mather, I. Black, K. Baker, and D. M. Paterson, Measuring *in situ* erosion shear stress of intertidal sediments with the Cohesive Strength Meter, *Estuarine, Coastal and Shelf Processes, 49*, 281-294, 1999.

Torres, R., M. J. Mwamba, and M. A. Goni, Properties of intertidal sediment mobilized by rainfall, *Limnology and Oceanography, 48*(3), 1245-1253, 2003.

Vogel, R. L., B. Kjerfve, and L. R. Gardner, Inorganic sediment budget for the North Inlet Salt Marsh, South Carolina, USA, *Mangroves and Salt Marshes, 1*(1), 23-25, 1996.

Voulgaris G., and S. Meyers, Net effect of rainfall activity on salt marsh sediment distribution, *Marine Geology*, in press, 2004.

Ward, L. G., Suspended-material transport in marsh tidal channels, Kiawah Island, South Carolina, *Marine Geology, 40*, 139-154, 1981.

Woodin, S. A., R. L. Marinelli, and S. M. Lindsay, Process-specific cues for recruitment in sedimentary environments: Geochemical signals?, *Journal of Marine Research, 56*, 535-558, 1998.

Woodin, S. A., D. S. Wethey, and S. M. Lindsay, Process specific recruitment cues in marine sedimentary systems, *Biol. Bull., 189*, 49-58, 1995.